Enhanced Field Emission from Chemically Etched and Electropolished Broad-area Niobium

Tong Wang

Virginia Tech, Blacksburg, VA 24061 USA

Charles E. Reece and Ronald M. Sundelin

Thomas Jefferson National Accelerator Facility, Newport News, VA 23606 USA

Electron field emission (FE) from broad-area metal surfaces is known to occur at a much lower electric field than predicted by the Fowler-Nordheim law. This enhanced field emission (EFE) presents a major impediment to high electric field operation in a variety of applications, e.g., in superconducting niobium radio-frequency cavities for particle accelerators, klystrons, and a wide range of high voltage vacuum devices. Therefore EFE has been the subject of wide fundamental research for years. Although micron or submicron particles are often observed at such EFE sites, the strength and number of emitting sites and the causes of EFE strongly depend on surface preparation and handling, and the physical mechanism of EFE remains unknown. To systematically investigate the sources of this emission and to evaluate the best available surface preparation techniques with respect to resulting field emission, a DC scanning field emission microscope (SFEM) has been built at Thomas Jefferson National Accelerator Facility (Jefferson Lab). Broad-area samples can be moved laterally in a raster pattern (2.5 μm step resolution) under a high voltage micro-tip for EFE detection and

localization in the SFEM. The emitting sites can then be characterized by SEM and EDX without breaking ultra high vacuum. EFE sources from planar Nb have been studied after preparation by chemical etching and electropolishing combined with ultrasonic de-ionized water rinse (UWR). Emitters have been identified and analyzed, and the preparation process has been refined and improved based on scan results. With the improved preparation process, field-emission-free or near field-emission-free surfaces at ~140 MV/m have been achieved consistently on a number of samples.

61.16.Fk, 79.70.+q

Introduction

Enhanced field emission (EFE) is a fundamental limitation in a wide range of high voltage vacuum devices, for instance, x-ray tubes, electron microscopes, power vacuum switches, klystrons and high-field superconducting radio-frequency (SRF) niobium (Nb) resonators for particle accelerators.[1 2 3] Field emission, when utilized as a source of electrons in cold cathode devices, has applications in flat panel displays, microwave cathodes and other cathodes, micro-electro-mechanical systems (MEMS), solar conversion and other devices. Since the fundamental mechanism of EFE is not expected to differ significantly from one solid metal to another, the conclusions obtained from niobium in this work are expected to be applicable to other material as well.

Field emission of electrons occurs when electrons tunnel through the surface barrier of a metal into vacuum under high electric field. The emission from a clean metal surface was explained by Fowler and Nordheim in terms of a quantum mechanical tunneling effect in 1928.[4 5] The result is the so-called Fowler-Nordheim (F-N) law:

$$j = \frac{A \times E^2}{\phi} \times \exp\left(-\frac{B \times \phi^{\frac{3}{2}}}{E}\right), \qquad (1)$$

with $A = 1.54\times10^{-6}$, $B = 6.83\times10^{7}$, current density j in A/cm^2, electric field E in V/cm and work function ϕ in eV ($\phi = 4$ eV for Nb). In practice, FE current is measured at fields much lower than that described by the F-N law on a clean metallic surface, and this phenomenon is called Enhanced Field Emission. In order to interpret EFE by the F-N law, a field enhancement factor β (> 1) is introduced and usually leads to a good approximation by the modified Fowler-Nordheim equation, i.e.,

$$I = \frac{A\times S\times \beta^2 \times E^2}{\phi}\times \exp(-B\times\frac{\phi^{\frac{3}{2}}}{\beta\times E}), \qquad (2)$$

with local field enhancement factor β (generally ranges from 50 to 1000), effective emitting area S in cm^2 (generally ranging between $10^{-14} - 10^{-5}$). Reviews exist on this subject.[6 7]

Field emission research on a variety of material, such as Cu, Ni, stainless steel, Ti, Mo, W, etc. has been conducted around the world. Focusing on the material used for SRF cavities in particle accelerators, Nb, and other relevant material, a number of institutions has conducted research in FE as follows. Ph. Niedermann from University of Geneva was among the first to carry out an extensive study on Nb using a DC field emission scanning apparatus which combined FE scanning with *in situ* microscopic observation and material characterization of emitters.[8] The University of Wuppertal built a similar apparatus to that of the University of Geneva and conducted research on Nb, Cu, Al, diamond films, etc.[9] Researchers at Centre d'Etudes de Saclay (Saclay) and Institut de Physique Nucleaire (IPN) Orsay, France modified a commercial Scanning Electron Microscope (SEM) to a FE scanning apparatus at the nA level and also built a sensitive device to detect FE current well below 1 nA.[10] Material they have investigated includes Nb, Cu and

Au. Cornell University examined the inner surface of an SRF Nb cavity after the occurrence of field emission. They also built a special "mushroom" shaped cavity to test FE on Nb samples mounted inside of the cavity, and the sample could then be detached for SEM observation and material characterization.[11] Results from the above research show that EFE sources are localized micron or submicron sites, and many appeared to be particles or geometrical scratches/damage. Most emitters contain foreign elements, although the types of elements differ.[8 9] Some models were proposed to explain EFE, including a geometrical enhancement (protrusion) model,[12] a metal-insulator-vacuum (MIV) model,[7 13 14 15] etc. The bulk of studied emission sites are most probably external instead of intrinsic due to the non-standard preparation and handling procedures. FE reduction achieved by the above institutions are summarized in Figure 9. All of the above studies on Nb have been discontinued to the authors' knowledge.

The experimental objectives of this work are as follows. (1) To design and build an ultra high vacuum DC field emission scanning apparatus capable of locating individual emitters on Nb and of providing *in situ* microscopic characterization. (2) To conduct a systematic study of field emission sources on Nb with respect to the best available cleaning techniques, i.e., chemical etching by buffered chemical polishing (BCP) and electropolishing. (3) To establish a preparation process to minimize field emission, as this will leave emitter sources that are more intrinsic to the material and are ready for further studies. Only through this systematic approach can we overcome the reproducibility problems encountered in field emission performance from Nb cavities and Nb samples. (4) To devise a methodology to distinguish external particles from intrinsic impurities as this will provide information on the directions in which effort is needed for their removal.

(The definition of external emitters and intrinsic emitters will be given in the following paragraph). (5) To gain some information and understanding in regards to the physical mechanism of enhanced field emission from their microscopic appearances and elemental compositions.

External emitters, a term that when used in this paper refers to geometrical damage (scratches, etc.) and foreign particles coming from handling and machining, have been evidenced by past experimental results. Intrinsic emitters, a term that when used in this paper refers to grain boundary and material bulk impurity, were suggested to be possible emitters because of the local geometrical field enhancement at grain boundaries or evidence from early experimental work,[16] but have not been experimentally confirmed or refuted for naturally occurring emitters on high purity contemporary metal surfaces. The categories of known and potential emitters on material surfaces are schematically illustrated in Figure 1. True F-N field emission, which occurs at above the GV/m level, and is sometimes also referred to as intrinsic emission, should not be confused with the intrinsic emission definition in this work, i.e., for this paper, all FE refers to EFE unless noted otherwise.

Experimental Apparatus and Procedures

Experimental Apparatus

We designed and built an apparatus, termed a Scanning Field Emission Microscope (SFEM). The detail of the apparatus was described by the authors (refer to reference [17]). The main structure and functions are as follows. It is a UHV device (~10^{-9} Torr), attached through a UHV bellow and a gate valve to an Amray Scanning Electron Microscope (SEM 1830) with a nominal resolution of several nm. A heat treatment (HT) chamber is attached to the SFEM by a gate valve, as shown in Figure 2. Samples are loaded via the SEM, and can be transferred under vacuum to the other two chambers by a hermetic retractable linear rotary transporter (travel range: 914 mm).

Within the SFEM chamber, samples of slightly larger than 25 mm diameter can be moved in x, y, and z under an anode tip by a motorized high precision sample manipulator. The resolution of sample manipulation in x, y, and z is 2.5 μm, and the travel range in the x, y plane is a circle of 25 mm diameter. Tungsten anode tips are mounted on a high voltage anode holder that can be moved linearly for tip exchange. An anode of 150 μm radius (cylindrical tip) and anodes of 10 and 1 μm tip curvature radius (paraboloid shaped) can be selected for coarse, medium and fine scans. After emitters are accurately located in the SFEM chamber, the sample is transferred to the SEM chamber for emitter characterization. The SEM is equipped with Energy Dispersive X-ray Spectrometer (EDS) capable of windowless operation for light element sensitivity.

Three artificial marks on each sample surface are used as fiducials to calculate the x, y coordinates of emitters in the SEM chamber from their coordinates in the SFEM chamber. The resulting common accuracy in re-locating emitters under SEM is ±100–200 μm. As the sample preparation process is progressively refined and controlled, the

number of emitters per sample has dropped to 1–2/sample, as will be addressed in following sections. With the low number of emitters, and the fact that the ±500 μm area around the calculated emitter location is always closely examined for any micron or submicron scale features under the SEM, the identification of emitters is routinely unambiguous, and can often be further confirmed by a second FE scan after an ultrasonic water rinse to remove the suspected emitting particle.

The HT chamber is designed for the purpose of sample outgassing by external radiation and sample thermal processing by electron bombardment up to 1400°C. The apparatus is located in a Class 1000 cleanroom to reduce the risk of contamination by air-borne dust during sample handling.

The sample and sample holders in all three chambers, i.e., SEM, SFEM, and HT, are specially designed for the sample to have self-alignment capability in the sample holder, i.e., every point on the sample surface can return to its previous position after non–*in situ* processing. The repeatability in x, y is proven to be ~140 μm or better. With the additional aid of surrounding grain shapes as seen with the SEM, this design facilitates the relocation of micron to submicron features after non–*in situ* as well as *in situ* preparation (and also provides a way to experimentally determine the origin of emitters, i.e., external particles or material bulk impurities, after a second water rinse.)

Experimental circuit and procedures

The electronic circuit for the experiment is illustrated in Figure 3. The high voltage power supply is controlled by a computer with a data acquisition card to output a voltage ramp from 0 up to 40 kV (depending on the electric field chosen for the field emission scan) in steps of +200 V, or until a field emission current threshold, usually set at 1–2 nA above the displacement current, is reached, detected by a picoammeter. The displacement current is constant during ramping and is due to the gap capacitance between anode tip and sample, and the voltage ramp. Once the threshold current is reached, the computer will abort the voltage ramp and the maximum voltage that is reached at the anode is recorded to depict the emitting field of the emitter. Hence, detection of strong and weak emitters is accomplished in a single scan. The high resistance (100 GΩ) high voltage resistor is custom-made to be vacuum compatible and is placed inside the vacuum chamber in order to reduce the ability of the energy stored in the cable capacitance to damage or destroy emitters during a vacuum arc.

The gap between anode tip and sample (usually set at 100–200 μm, depending on the electric field chosen for field emission scan,) during each scan is maintained by adjusting the sample position in z while moving in x, y according to the mean surface plane. The mean surface plane is obtained by fitting multi-point profile data for each sample surface. The multi-point profile data are obtained by moving the sample up in z until it slightly touches the anode tip at the selected points, indicated by a short circuit between sample and anode tip. This method results in a gap consistency of about ±10 μm determined from a long distance optical microscope.

The FE scan on an entire surface can be done using anode of 150 or 10 μm tip radius for coarse to medium resolution scan. After emitters are located, a local fine scan around the emission sites using anode of 1 μm tip radius at a gap of 50 μm will accurately locate the emission center. Electric field at the cathode directly below anode tip, E, is dependent on anode shape, tip radius and gap distance. The electric field correction factor κ (= V/Ed) can be calculated based on Ph. Niedermann's analysis for paraboloid shaped and hyperboloid shaped anodes,[8] with V as the applied anode voltage, d as the gap distance from anode apex to cathode plane. For parallel plane geometry (curvature radius $r >> d$), $\kappa \cong 1$. For various anode and gap configuration in our experiment, κ is calculated accordingly and verified in parallel plane geometry (ranging from 1–3).

The gap can be calibrated at the emitter by centering the anode at the emission center and gradually reducing the gap, e.g., from 50 μm to 10 μm, while adjusting the high voltage to maintain a constant current. $V(d)$ follows a linear trend, and the extrapolation of $V(d)$ plot to $V = 0$ is set as gap = 0. The slope of the fitted straight line divided by the correction factor κ gives the calibrated electric field.

To characterize an individual emitter, the field enhancement factor β and effective emitting area S can be obtained by linear fitting of $\ln(I/E^2)$ versus $1/E$. (Refer to Equation (2).) .) An illustration of F-N plot is shown in Figure 4.

The experiment, including entire surface scan and characterization of individual emitters, is automated using the data acquisition computer.

Field emission from chemically etched Nb

Field emission from initial samples

The present EFE study is made on bulk Nb surfaces such as are used in SRF resonating cavities employed in particle accelerators. In the same manner as is done with Nb cavities, a number of Nb samples made from high purity (RRR~300, where RRR is the ratio of resistance at room temperature to that at low temperature (normal state)) Nb sheet were chemically etched by BCP (buffered chemical polish, HF (49%) : HNO_3 (69%) : H_3PO_4 (85%) = 1:1:1) to remove the machining damage layer. To remove acid residue and particles on samples introduced during handling, ultrasonic cleaning in de-ionized water was performed immediately following BCP. Some samples were blown dry by filtered nitrogen gas, while others were methanol rinsed to displace water from the surface, and then placed on a filtered laminar flow bench in the cleanroom for a few minutes until dry.

About 20 Nb samples were BCP etched for various amounts of surface removal and scanned for field emitters at ~70 or 140 MV/m. Generally, five types of emitters were located: geometrical damage (scratches), particles containing foreign elements, features which appear to be non-particle-like using the SEM and with no foreign elements detectable by EDS (possibly due to the relatively large probing depth of EDS compared to that of SEM), geometrical irregularities that may have been caused by the non-

uniformity of etching, and emitters with no distinctive or resolvable features. There were also sites that were completely destroyed by vacuum arcs. Although they may not all be field emission initiated, they will be listed as a category of emitters in this paper—emitters destroyed by vacuum arc—for simplicity.

In order to reduce emitters caused by geometrical damage, precautions in sample handling were taken to make sure that the surface is never touched by any means after BCP. After this change, this category of emitters was reduced to zero after a sufficient amount of removal by BCP, but the other five categories of emitters remain. Furthermore, even with a similar and significant amount of removal, emitter density still varies significantly from one sample to another, for example, a total of 8 emitters for the best sample, and over 60 emitters for the worst. A selection of SEM pictures for different categories of emitters is shown in Figure 5. The majority of emitters, however, are foreign particles or contaminants, with various elemental compositions.

The majority of emitters from the ~20 samples were located and analyzed. A subset of these emitters were characterized according to the modified F-N parameterization for their geometrical enhancement factors, β, and effective emitting areas, S. A small selection of these emitters are listed in Table 1.

Field emission after machining improvement

In order to overcome the reproducibility problem encountered previously in field emission performance, the machining process was examined first, as Nb is a soft, abrasive metal whose machining process is not easily controlled. A few rules, as listed below, were proposed and followed for new samples.

- inspect Nb sheet to choose defect-free material
- use a designated clean area for the machining
- use only plastic fixtures in the machining to minimize the damage to the sample surface
- change machining tools frequently as dull tools will embed impurities into the sample

New samples were made from a Nb sheet of ~300 RRR that was closely examined to be free of visible defects. They were then BCP etched to remove various amounts of material from the surfaces, followed by ultrasonic rinse in de-ionized water (UWR). Finally, samples were methanol rinsed and laminar air-flow dried in a cleanroom before being scanned for field emission. The results at ~140 MV/m are listed in Table 2.

The previous five categories of emitters now have dropped to three, i.e., geometrical irregularities and emitters with no discernible features were not found from this group of samples, which indicates that these emitters might be related to the previous sample surfaces that were not quite contaminant-free. For instance, the non-uniform chemical etching at contaminated sites could cause the geometrical irregularities or etch pits, while traces of contaminant embedded at grain boundaries could cause field emission whose source is impossible or very difficult to identify.

Seven of the nine foreign particulate emitters contain Fe, Cr and Ni or a subset of these elements, along with Nb and other foreign elements. They could originate from machining tools made of stainless steel. The rest of the emitters contain Ag and Nb, and Nb respectively. They emit at a wide range of electric fields, from 40 MV/m up to 140 MV/m. They are categorized as foreign particles because of their appearances and/or the fact that they are completely or partly washed away by further ultrasonic water rinsing. The sample edges, although not within the FE scan area, are found to have many machining damage sites and contaminants under SEM and EDS. These contaminants could be a source for the identified particulate emitters rich in stainless steel, e.g., if they are rinsed off into the water medium by ultrasonic rinsing and then re-deposited onto the sample surfaces. As a result, further improvement in machining was pursued to reduce this category of field emitters, which will be described in the following section.

Emitters were also found that appear bright but not particle-like under the SEM and do not have any foreign elements detected by EDS. The several micron profiling depth of EDS makes it unsuitable to detect very superficial elements. The last category of emitters are those completely destroyed by vacuum arcs. These often occurred at fields similar to the emitting fields of foreign particles, but EDS analysis indicated no foreign elements at arc sites, possibly due to vaporization of foreign elements. One should note that some microparticles caused a vacuum arc but weren't completely destroyed by it, and therefore can be studied to confirm the existence of foreign elements and are listed as foreign particles in the first category. The possible causes of vacuum arcs will be discussed later in the paper.

As shown in Table 2, the emitter density is significantly reduced to $28/(6\times4.9\ cm^2) = 0.95/cm^2$, and is reasonably repeatable from sample to sample. Further BCP removal doesn't monotonically reduce the emitter density on the same sample, i.e., observed emitter density is independent of BCP removal of additional Nb, which indicates that the damage layer is already removed from the surface area. Therefore, a fresh new surface was studied each time in subsequent BCPs and treated as if it were a new sample in the statistics. Some SEM pictures of the above emitters are shown in Figure 6 along with emitters from the next section.

Field emission after further improvement in sample preparation

In an effort to further reduce the emitter density and to control the damage extent of vacuum arcs, improvement in sample preparation and in the experimental circuit was made as follows. Several new samples were cut from the same Nb sheet as was used for samples listed in Table 2, but were made larger so that the field emission scan can be even further away from the edge area, which is prone to have machining contaminants. The previous 1 GΩ current-limiting resistor was changed to the present 100 GΩ to further reduce the damage of vacuum arcs and hopefully to preserve the arcing sources for studies. Field emitters subsequently detected in ~140 MV/m scans are shown in Table 3.

As illustrated in Table 3, a repeatable emitter density (averaged at $8/(7\times4.9\ cm^2) \cong 0.23/cm^2$) has been achieved in this series of tests at ~140 MV/m, reduced by ~75% from the value calculated from Table 2. This is the lowest emitter density ever achieved on Nb samples at the highest field, and it will be discussed in more detail in the following sections.

Foreign particles were found to emit over a wide range of electric fields (from 35 to 100 MV/m) in this series of tests, similar to previous results. One of the emitters contains Nb, Fe, Ti, Ca. Sample #75-2 is emission free up to 99 MV/m, and sample #81-1 is emission free up to 140 MV/m. SEM pictures of some of the emitters in Table 3 along with selected emitters listed in Table 2 are shown in Figure 6.

Discussion

Comparing Table 3 with Table 2, not only are un-destroyed emitters reduced from 14/6 ($\cong$ 2.33) per sample to 3/7 (=0.43) per sample, but also the occurrence of vacuum arcs are further reduced from 14/6 ($\cong$ 2.33) to 5/7 ($\cong$ 0.71) per sample, which indicates that machining contaminant was indeed and may still be the main source of particulate emitters and vacuum arcs, hence may represent the key step in reducing field emission. Other possible sources for the remaining emitters are dust particles from inside the vacuum chamber being stirred up by opening or closing the gate valves, or airborne dust particles in the cleanroom falling onto a sample surface during the transfer from the laminar bench to the SEM chamber. A better controlled environment, such as a class 100

or 10 cleanroom may be better suited to achieving further reduction in field emitter density. Whether the foreign particles were caused by operating the gate valves needs to be investigated in possible future experiments.

Vacuum arcs or sparks—transient vacuum breakdown within the gap—are observed with the optical microscope. The mechanisms that initiate vacuum arcs are very complex, and some may evolve from an initial field emission while some may not, as described in Latham's book.[7] Many theories for cathode-initiated arcs are based on the initial heating of the cathode emitter to reach thermal instability, which is unlikely for an intrinsic emitter because of the good thermal contact with the bulk material. In the mean-time, the physical transfer of weakly-bound microparticles from cathode to anode or vice versa, due to pure mechanical forces from a strong electric field, has been proved by experiments to initiate a breakdown. As described in the previous section, foreign particles were found at the center of some arc sites, which proved that foreign particles can start a breakdown, regardless of whether field emission is involved in the process. Furthermore, the fact that the average number of vacuum arcs per sample can be further reduced to ~3/10 of the previous value in Table 2 also strengthens the authors' view that they are less likely caused by intrinsic emitters, which should largely remain unchanged in number, since all the samples were cut from the same Nb sheet.

Field emission from electropolished Nb

Field emission results from electropolished samples

Electropolishing is also called electrolytic polishing. The specimen to be polished (anode) and a cathode made of a suitable material are immersed in an electrolyte and connected to a battery or power supply. Although the polishing mechanism is not yet completely understood, it is believed that a viscous liquid layer immediately adjacent to the specimen surface is critical in the "smoothing" effect of electropolishing.[18] The electropolishing method developed by the Siemens company is often used for Nb cavities.[19] The electrolyte formula consists of 850 ml sulfuric acid (96%) and 100 ml hydrofluoric acid (40%). The cathode is normally made of pure aluminum.

The resulting Nb surface is very smooth and shiny compared to the surface conditions obtained by BCP. A comparison of the typical grain boundary geometry for the two types of surfaces measured by R. Sundelin is shown in Figure 7.[20]

After the tests listed in Table 2, sample #65 and #63 were BCP etched to remove another 80 μm, then electropolished to remove ~40 μm. Sample #61 of the same size was BCP etched to remove 330 μm in total, then also electropolished to remove an additional 40 μm. Subsequently, the samples were ultrasonic cleaned in de-ionized water and then briefly rinsed in methanol followed by laminar air drying in the cleanroom. The field emission scan results at ~140 MV/m are shown in Table 4.

The emitter categories are the same as for BCP samples: foreign particles and emitters destroyed by vacuum arc. No difference caused by chemistry is observed. The only

foreign particulate emitter found in these tests, which caused a vacuum arc but wasn't destroyed by it, contains Nb, Fe, and Cr. As discussed before, it could be re-deposited contaminant from stainless steel machining tools. Its SEM picture is shown in Figure 8 (the nearby craters are caused by vacuum arc). An emission free surface is achieved on #65-4 up to 105 MV/m. The average emitter density of $6/(3\times4.9\ cm^2) \cong 0.4/cm^2$, is lower than corresponding BCP samples in Table 2 ($0.95/cm^2$). However, the low base number of emitters makes it difficult to statistically state that electropolishing is better than chemical etching with respect to FE suppression, i.e., that the smoother surface resulted from electropolishing makes particle removal more effective.

Discussion and Conclusion

Observation and discussion

All located emitters appeared to be conducting and in electrical contact with the Nb sample (no charging in SEM), which is in favor of the geometrical enhancement model. However, the majority of them contain foreign elements, and appear bright in SEM (due to the higher secondary electron yield from insulator than metal), and many emitters lack the necessary sharp protrusion for emission to occur. Tiny round melted particles of Nb and W (from anode) generated from vacuum arcing occasionally can become new emitters, even though often at ~100 MV/m or higher. The discrepancy in geometrical factor is still not negligible, thus undermining the possibility that the geometrical

enhancement model represents the whole story (unless there are additional geometrical features that are below the resolution limit of the SEM). We occasionally also observed non-emitting conducting particles with appearances that are not too different from the emitting ones. Although all emitters identified in this work were found to be conducting, it could be that our sample preparation and handling environment didn't favor the presence of insulating particles.

Switching and hysteresis in I-V characteristics were observed on some emitters in this work, which favors some EFE models involving insulators,[7] but these emitters showed no significant distinction in their appearances or composition from other stable emitters.

Summary and conclusions

From the results presented above, the following conclusions are drawn:

(1) Undestroyed emitting sites are found to be foreign microparticles on chemically etched or electropolished Nb. They are proved most likely to be re-deposited machining contaminant originating from the sample edge. Other possibilities are dust from inside the vacuum chamber or airborne dust particles collecting on sample surfaces during transfer in the cleanroom. Further reduction would likely require a cleaner environment, e.g., Class 100 or 10 cleanroom for particle control.

(2) No intrinsic emitters have been observed up to 140 MV/m from chemically etched (scan area: ~64 cm^2) or electropolished samples (scan area: ~15 cm^2). This is somewhat

in disagreement with the University of Wuppertal's findings that emitter density increases with material bulk impurity content.[21] However, all of their localized emitters are particles containing Nb and Fe, consistent with the majority of the emitters from our samples, which in our case were later removed by improving the machining process and sample preparation, and thus their identified emitters may not be bulk impurities. Nonetheless, the trend of emitter density increasing with material impurity grade may still be true, only that at RRR~300, the density of impurity conglomerate is low enough to approach zero for the sample area that we examined (80 cm^2 from 16 samples listed in Table 2, 3, 4), or the impurity will only become emitters at higher fields.

(3) No inherent difference in emitter nature due to different chemistry, nor significant difference in emission density, is observed up to 140 MV/m between chemically etched and electropolished Nb.

(4) The lowest emitter plus vacuum arc density ever achieved in a DC field emission scanning apparatus, i.e., 0.23/cm^2, and at the highest field of 140 MV/m, is achieved by chemical etching and ultrasonic rinse from each of a series of tests without exception. The statistical comparison with other institutions is shown in Figure 9. Emission free samples up to ~100 MV/m were achieved by BCP (#75-2) and EP (#65-4) with ultrasonic rinse. Emission free up to 140 MV/m was achieved by BCP and ultrasonic rinse (sample #81-1).

(5) Reproducible and maximal reduction in FE for a variety of applications can be presumably achieved by: improving the material machining process, which is often

overlooked but shown to be critical by this work; carefully controlling the chemical etching and cleaning process; and stringent particle control afterwards to prevent re-contamination.

Acknowledgment

The authors would like to thank Larry Phillips for his help with the apparatus, Brett Lewis and Tom Goodman for their assistance with the maintenance of the SEM, and Fred Dylla for his careful review of the manuscript.

* This work was supported by the U.S. DOE Contract No. DE-AC05-84ER40150.

Table 1: A small selection of analyzed emitters from the initial ~20 samples after 150 μm - 450 μm removal by buffered chemical polishing (BCP) unless otherwise noted (EP: electropolishing). #9-1(3), e.g., is from sample #9, after the 1st surface removal (2nd, 3rd,..... is after additional removal), on emitting site No. 3). Indicated fields are the fields that yield 2 nA field emission current throughout this paper.

Emitter	Emitting field (MV/m)	Elements detected by EDS	β	S (cm^{-2})
#9-1(3)	56	Nb	202	4.7E-13
#9-1(4)	56	Nb	180	1.6E-13
#7-1(46)	103	Nb,Fe,Al		
#8-1(2)	89	Al,Si,Ca, Ba,Nb		
#8-1(39)	47	Nb,Fe		
#25-1(1)	93	Nb,Fe,Cr, Ni,Mn		
#25-1(5)	135	Nb,Ca		
#25-1(8)	117	Nb,C		
#25-1(39)	135	Nb,Fe		
#32-1(1)	93	Nb,Fe,Cr,Ni		
#32-1(2)	47	Nb,Cr,Fe, Ni,Si		
#32-1(10)	117	Nb,Fe,Cr,Ni		
#32-1(11)	51	Nb,Cr,Fe,Ni		
#32-1(14)	89	Nb,Ca,Al, Zn,Fe,C		
#32-1(17)	70	Nb,Cu		
#34-1(1)-EP	34	Nb,Fe		
#34-1(2)-EP	33	Nb,Fe,Cr,Ni		
#34-1(3)-EP	19	Nb,Fe,Cr,Ni		
#34-2(1)	140	Nb,Fe		
#34-2(15)	95	Nb,Fe		
#54-1(1)	46	Nb	87	1.5E-12
#54-1(2)	94	Nb,Ca,Si, Al,C,Zn	34	8.26E-11

Table 2: Field emitters from BCP samples after improvement in cleanliness of the machining procedures (Field emission scanning field is 140 MV/m. Indicated fields are the fields that yield 2 nA FE current. The scan area for each sample is 25 mm dia.).

Sample No.-nth test (total surface removal by BCP)	Foreign particles	Features with Nb detected only	Emitters destroyed by vacuum arc
#65-1 (250 μm)	2 [40 MV/m (Nb, C, Cu, Ca, Fe, Ni), 86 MV/m (Nb, W, Ni, O)]	0	1
#65-2 (280 μm)	2 [140 MV/m (Nb, Fe), 114 MV/m (Nb, Fe, Cr)]	3 [130 MV/m, 118 MV/m, 135 MV/m]	2
#65-3 (360 μm)	1 [136 MV/m (Nb, Fe, Cr, Ni)]	0	2
#63-1 (250 μm)	3 [100 MV/m (Nb, Fe, Cr), 42 MV/m (Ag, Nb), 105 MV/m (Nb, Fe, Cr)]	1 [133 MV/m]	4
#63-2 (330 μm)	0	1 [127 MV/m]	4
#66-1 (330 μm)	1 [120 MV/m (Nb)]	0	1

Table 3: Field emission results at ~140 MV/m from BCP prepared samples after further improvement in sample preparation. (Indicated fields are the fields that yield 2 nA FE current. The scan area for each sample is 25 mm dia.)

Sample No.-nth test (total surface removal by BCP)	Foreign particles	Emitters destroyed by vacuum arc
#75-1 (250 μm)	1 [35 MV/m (Nb, Fe, Ti, Ca)]	0
#75-2 (300 μm)	2 [99 MV/m (Nb), 103 MV/m (Nb)]	0
#72-1 (250 μm)	0	1
#72-2 (300 μm)	0	1
#76-1 (250 μm)	0	1
#81-1 (200 μm)	0	0
#83-1 (200 μm)	0	2

Table 4: Field emission results from electropolished Nb samples (scanning field ~140 MV/m. Indicated fields are the fields that yield 2 nA FE current. Scan area per sample is 25 mm dia.).

Sample No.-nth test (total surface removal)	Foreign particles	Emitters destroyed by vacuum arc
#65-4 (440 μm by BCP + 40 μm by EP)	1 [105 MV/m (Nb, Fe, Cr)]	0
#61-1 (330 μm by BCP + 40 μm by EP)	0	1
#63-3 (410 μm by BCP + 40 μm by EP)	0	4

List of table captions

Table 1: A small selection of analyzed emitters from the initial ~20 samples after 150 μm - 450 μm removal by buffered chemical polishing (BCP) unless otherwise noted (EP: electropolishing). #9-1(3), e.g., is from sample #9, after the 1st surface removal (2nd, 3rd,..... is after additional removal), on emitting site No. 3). Indicated fields are the emitting fields that yield 2 nA field emission current throughout this paper.

Table 2: Field emitters from BCP samples after improvement in cleanliness of the machining procedures (Field emission scanning field 140 MV/m. Indicated fields are the emitting fields that yield 2 nA FE current. The scan area for each sample is 25 mm dia.).

Table 3: Field emission results at ~140 MV/m from BCP prepared samples after further improvement in sample preparation. (Indicated fields are the emitting fields that yield 2 nA FE current. The scan area for each sample is 25 mm dia.)

Table 4: Field emission results from electropolished Nb samples (scanning field ~140 MV/m. Indicated fields are the emitting fields that yield 2 nA FE current. Scan area per sample is 25 mm dia.).

List of figure captions

Fig. 1 A schematic illustration of known and potential emitters on material surface.

Fig. 2 Experimental apparatus (top view).

Fig. 3 Experimental circuit diagram.

Fig. 4 β, S fitting for the characterization of emitter.

Fig. 5 A selection of field emitters from the initial Nb samples. (a) Nb, $\beta = 100$, S = 3E-13 cm^2, E = 57 MV/m. (b) Nb, Cr, Fe, Ni, E = 52 MV/m. (c) Nb, E = 62 MV/m. (d) Nb, $\beta = 180$, S = 1.6E-13 cm^2, E = 67 MV/m.

Fig. 6 A selection of field emitters from Table 2 and 3. (a) #63-1 (site 1), Nb, Fe, Cr, E = 100MV/m. (b) #66-1 (site 1), Nb, E = 119 MV/m. (c) #75-2 (site 2), Nb, E = 103 MV/m. (d) #75-1 (site 1), Nb, Fe, Ti, Ca, E = 35 MV/m.

Fig. 7 Comparison of grain boundary geometry for chemically polished and electropolished Nb.

Fig. 8 A foreign particle emitter from sample #65-1 prepared by electropolishing (The craters are caused by vacuum arc. The particle contains Nb, Fe, Cr. Its emitting field is 105 MV/m to extract 2 nA current).

Fig. 9 Density of field emission sites on Nb identified in DC (Geneva and Wuppertal) and RF studies (CERN and Cornell) (i.e., density of emitters with $E_{onset} \leq E_{pk}$ identified in a DC scan or an RF operation at E_{pk} surface field versus E_{pk}), with the addition of this work (JLAB).

[1] H. Padamsee, J. Knobloch, and T. Hays, *RF Superconductivity for Accelerators* (Wiley and Sons, New York, 1998).

[2] Proc. of the 7th Workshop on RF Superconductivity, CE Saclay, Gif sur Yvette, France, (1995), edited by B. Bonin

[3] Proc. of the 8th Workshop on RF Superconductivity, Padova, Italy, (1997).

[4] R. H. Fowler and L. Nordheim, Proc. Roy. Soc. London A 119, 173, (1928).

[5] L. Nordheim, Proc. Roy. Soc. London A 121, 626, (1928).

[6] R. J. Noer, Appl. Phys. A **28**, 1, (1982).

[7] R. V. Latham, *High Voltage Vacuum Insulation* (Academic Press, London, 1981)

[8] Ph. Niedermann, Ph. D thesis, University of Geneva, 1986.

[9] E. Mahner, G. Muller, H. Piel, and N. Pupeter, J. Vac. Sci. Technol. B **13 (2)**, 607, (1995).

[10] J. Tan, Proc. of the 7th Workshop on RF Superconductivity, CEA/Saclay, 105, (1995), edited by B. Bonin

[11] D. Moffat, P. Barnes, T. Flynn, J. Graber, L. Hand, W. Hartung, T. Hayes, J. Kirchgessner, J. Knobloch, R. Noer, H. Padamsee, D. Rubin, and J. Sears, Proc. of the 5th Workshop on RF Superconductivity, DESY, 245, (1991).

[12] H. H. Race, General Electric Review, 43, 365, (1940).

[13] R. V. Latham, Vacuum **32**, 137, (1982).

[14] C. S. Athwal and R. V. Latham, J. Phys. D: Appl. Phys. **17**, 1029, (1984).

[15] C. S. Athwal and R. V. Latham, Physica C **104**, 189, (1981).

[16] B. M. Cox, J. Phys. D: Appl. Phys. **8**, 2065, (1975).

[17] T. Wang, C. E. Reece, R. M. Sundelin, Rev. Sci. Instru., (2002), in press.

[18] T. Lyman, *Metals Handbook*, edited by T. Lyman, Vol. 8, Metallography, structure and phase diagram, (American Society for Metals, 8th edition, 1973), p. 26.

[19] H. Diepers, O. Schmidt, H. Martens, F. S. Sun, Phys. Letter. 37A. 139 (1971).

[20] R. Sundelin, E. von Borstel, J. Kirchgessner, D. Rice, and M. Tigner, IEEE Transactions on Nuclear Science, #3, Vol. NS-20, 98(1973).

[21] N, Pupeter, A. Göhl, T. Habermann, A. Kirschner, E. Mahner, G. Müller, H. Piel, Proc. of the 7th Workshop on RF Superconductivity, CE Saclay, Gif sur Yvette, France, (1995), edited by B. Bonin.

Fig.1 A schematic illustration of known and potential emitters on material surface.

Tong Wang, et al. Journal of Vacuum Science and Technology.

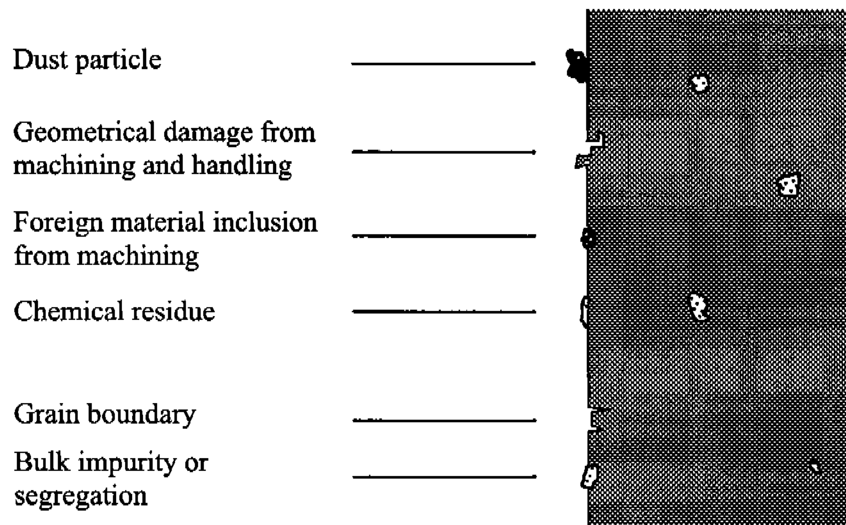

Fig. 2 Experimental apparatus (top view).

Tong Wang at al. Journal of Vacuum Science and Technology

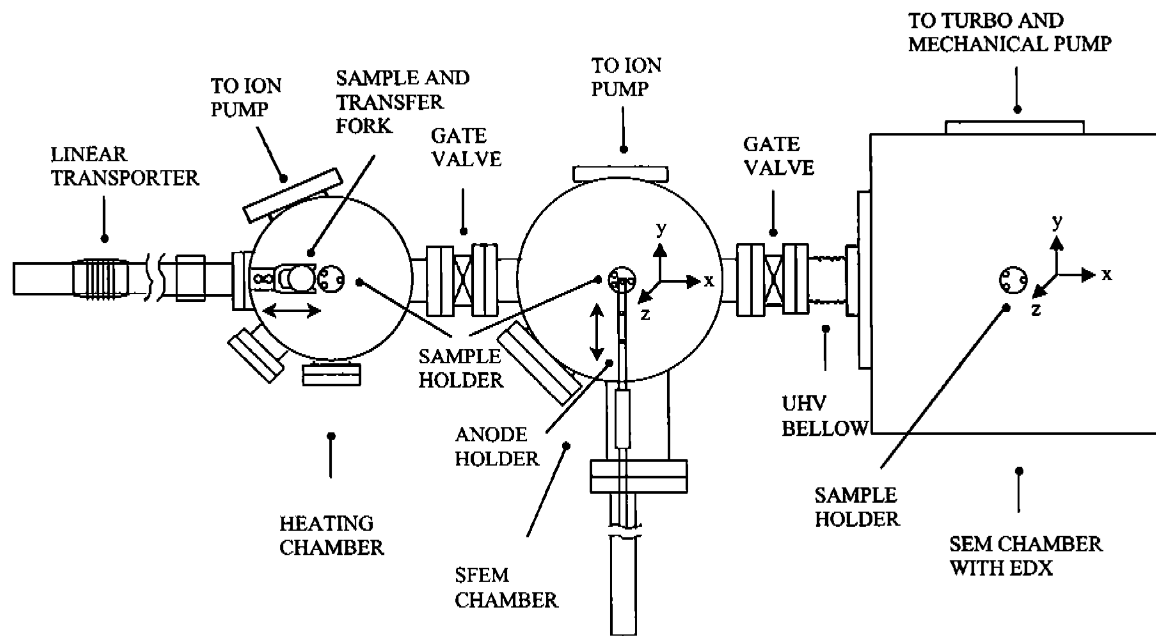

Fig. 3 Experimental circuit diagram

T. Wang, et al. Journal of Vacuum Science and Technology

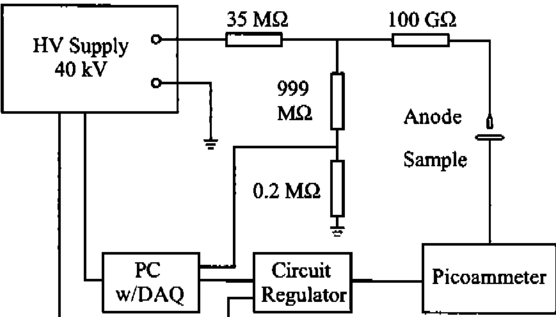

Fig. 4 β, S fitting for the characterization of emitter

Tong Wang, et al., Journal of Vacuum Science and Technology

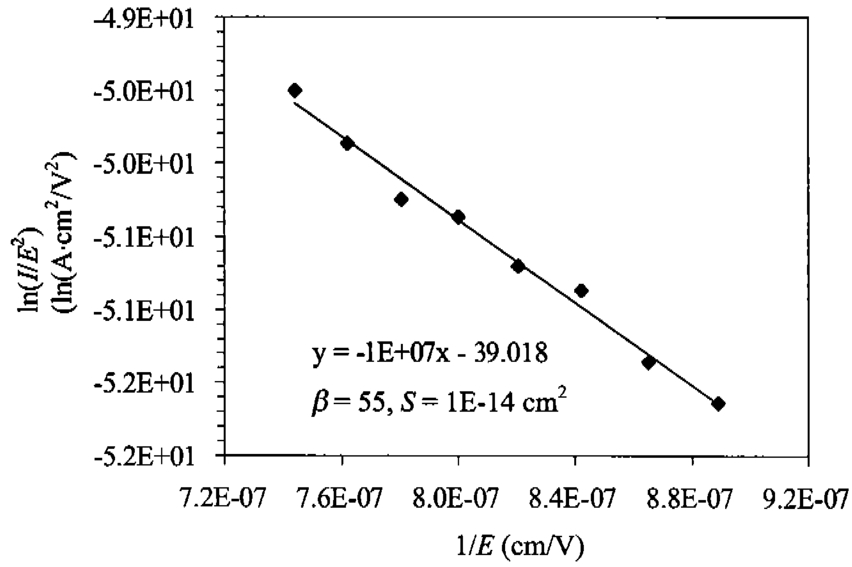

Fig. 5 A selection of field emitters from the initial Nb samples. (a) Nb, $\beta = 100$, S = 3E-13 cm^2, E = 57 MV/m. (b) Nb, Cr, Fe, Ni, E = 52 MV/m. (c) Nb, E = 62 MV/m. (d) Nb, $\beta = 180$, S = 1.6E-13 cm^2, E = 67 MV/m.

Tong Wang, et al, Journal of Vacuum Science and Technology

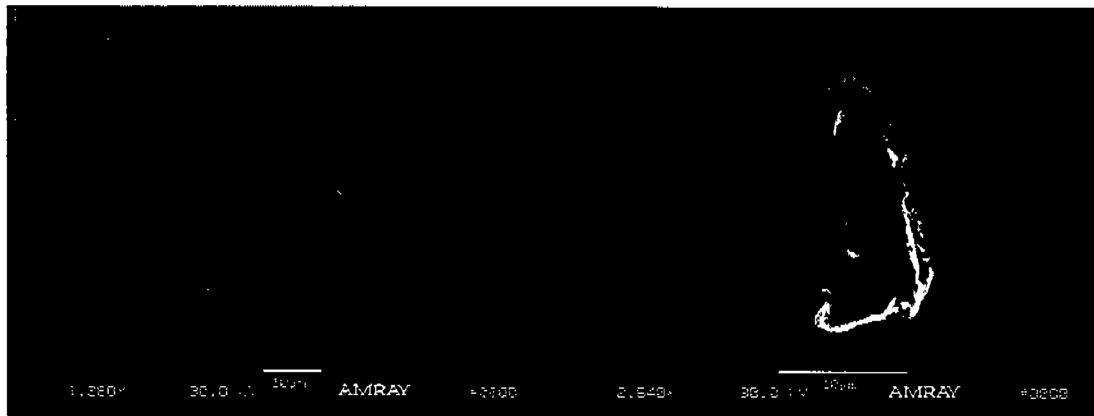

(a) (b)

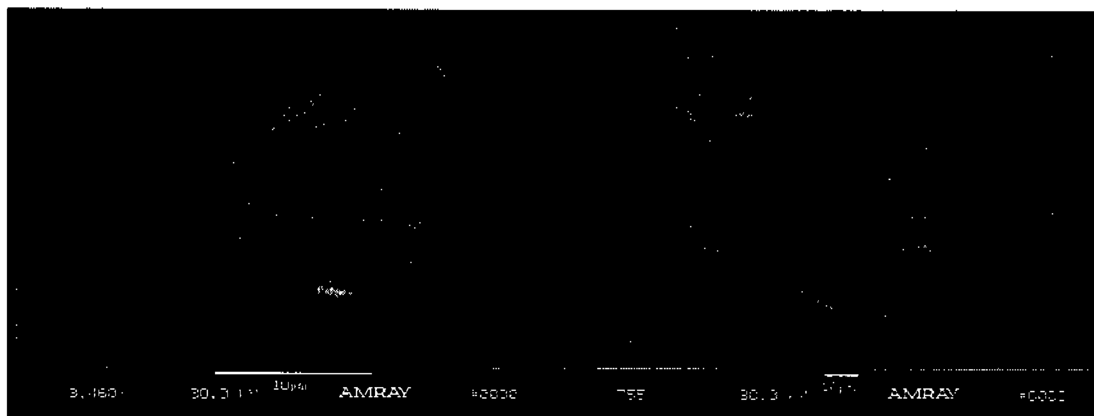

(c) (d)

Fig. 6 A selection of field emitters from Table 2 and 3. (a) #63-1 (site 1), Nb, Fe, Cr, E = 100MV/m. (b) #66-1 (site 1), Nb, E = 119 MV/m. (c) #75-2 (site 2), Nb, E = 103 MV/m. (d) #75-1 (site 1), Nb, Fe, Ti, Ca, E = 35 MV/m.

Tong Wang, et al, Journal of Vacuum Science and Technology

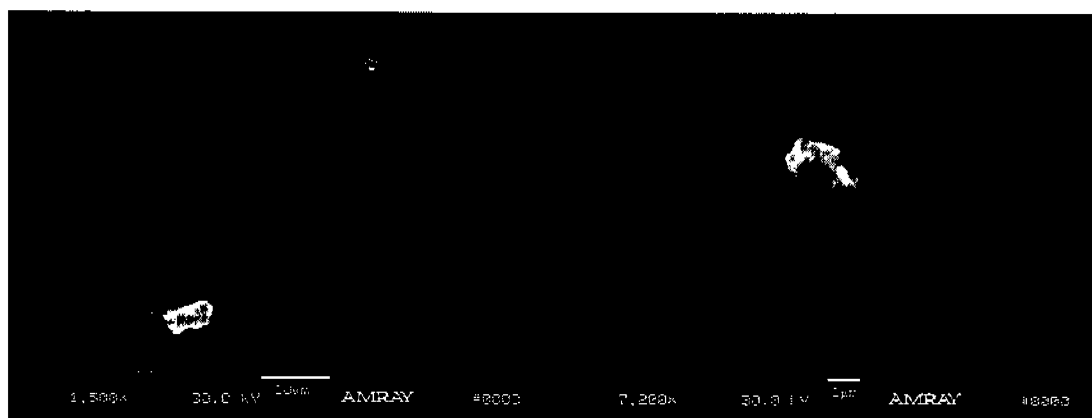

(a) (b)

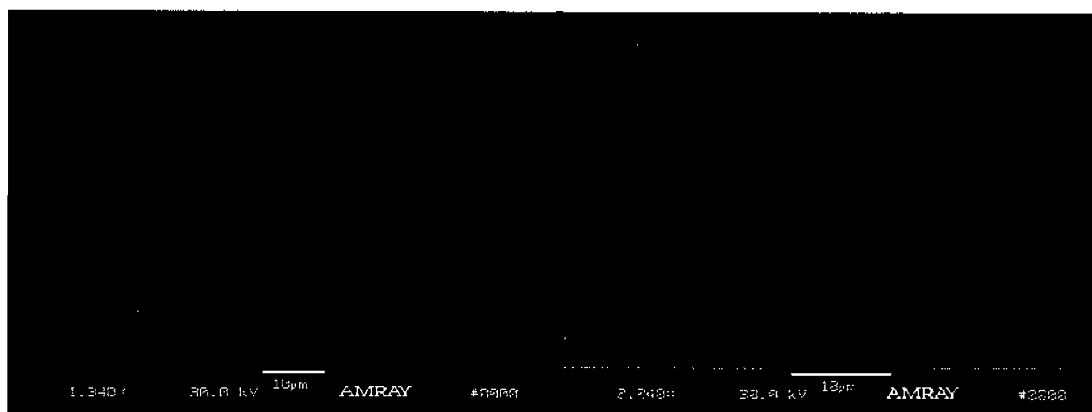

(c) (d)

Fig. 7 Comparison of grain boundary geometry for chemically polished and electropolished Nb.

Tong Wang, et al, Journal of Vacuum Science and Technology

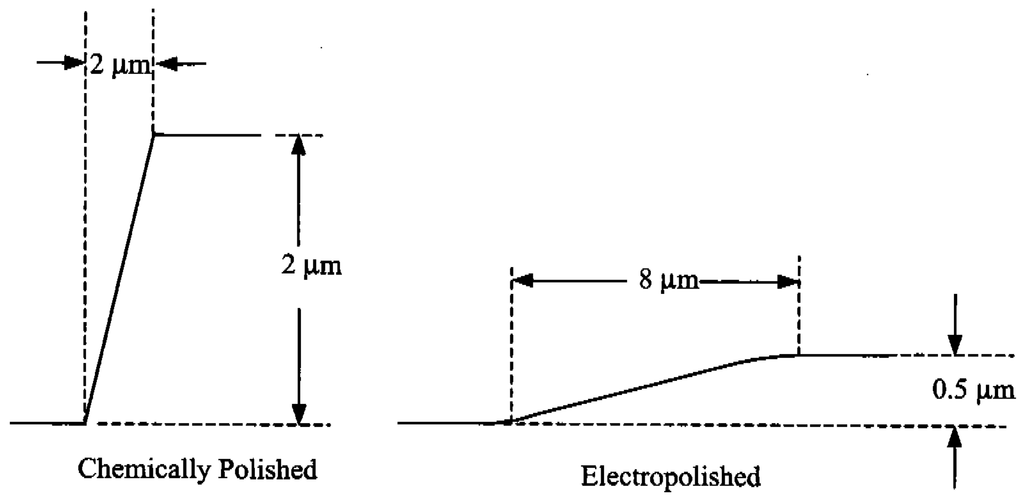

Fig. 8 A foreign particle emitter from sample #65-1 prepared by electropolishing (The craters are caused by vacuum arc. The particle contains Nb, Fe, Cr. Its emitting field is 105 MV/m to extract 2 nA current).

Tong Wang, et al, Journal of Vacuum Science and Technology

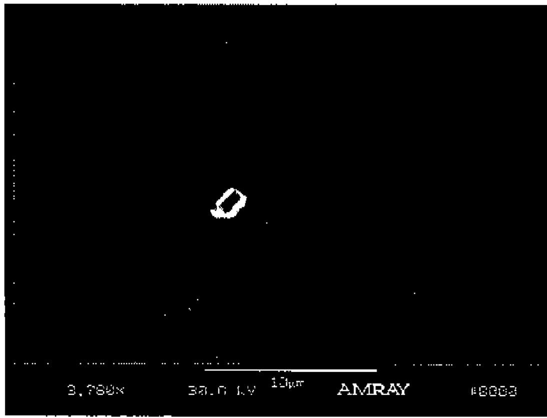

Fig. 9 Density of field emission sites on Nb identified in DC (Geneva and Wuppertal) and RF studies (CERN and Cornell) (i.e., density of emitters with $E_{onset} \leq E_{pk}$ identified in a DC scan or an RF operation at E_{pk} surface field versus E_{pk}), with the addition of this work (JLAB).

Tong Wang, et al, Journal of Vacuum Science and Technology